Film Cooling With Compound Angle Holes: Adiabatic Effectiveness

D. L. Schmidt

B. Sen

D. G. Bogard

Mechanical Engineering Department,
University of Texas at Austin,
Austin, TX 78712

Film cooling effectiveness was studied experimentally in a flat plate test facility with zero pressure gradient using a single row of inclined holes, which injected high-density, cryogenically cooled air. Round holes and holes with a diffusing expanded exit were directed laterally away from the free-stream direction with a compound angle of 60 deg. Comparisons were made with a baseline case of round holes aligned with the free stream. The effects of doubling the hole spacing to six hole diameters for each geometry were also examined. Experiments were performed at a density ratio of 1.6 with a range of blowing ratios from 0.5 to 2.5 and momentum flux ratios from 0.16 to 3.9. Lateral distributions of adiabatic effectiveness results were determined at streamwise distances from 3 D to 15 D downstream of the injection holes. All hole geometries had similar maximum spatially averaged effectiveness at a low momentum flux ratio of $I = 0.25$, but the round and expanded exit holes with compound angle had significantly greater effectiveness at larger momentum flux ratios. The compound angle holes with expanded exits had a much improved lateral distribution of coolant near the hole for all momentum flux ratios.

Introduction

Discrete hole film cooling is an important technique for cooling turbine blades in gas turbine engines. Much of the published research on the effectiveness of film cooling has concentrated on round holes, inclined at approximately 35 deg with respect to the surface, and aligned with the mainstream flow. In this work we used a flat plate test facility with zero pressure gradient to study the effectiveness of a single row of holes directed laterally away from the mainstream direction (i.e., with a nonzero compound angle). Two sets of laterally directed holes were studied; the first had round holes, and the second had holes with a circular metering section and a diffusing forward expansion at the exit of the holes (forward-expanded holes).

Compound angle injection has received renewed attention because this orientation is "believed to produce injectant distributions over surfaces giving better protection and higher film effectivenesses than injectant from holes with simple angle orientations" (Ligrani et al., 1992). However, there are few experimental or computational studies reported in the open literature. Experimental adiabatic effectiveness studies of laterally directed injection from a single row of holes into a zero pressure gradient flow over a flat plate are limited to those by Goldstein et al. (1970) for a single round hole with $\beta = 15$ and 35 deg, $CA = 90$ deg; Ligrani et al. (1992) for a single row of round holes with $\beta = 24$ deg, $CA = 50.5$ deg; and Honami et al. (1994) for a single row of round holes with $\beta = 30$ deg, $CA = 90$ deg. Honami et al. did not include streamwise-directed holes as a basis for comparison, but their near-hole compound angle effectiveness behavior was comparable to the other two studies. Compared to streamwise directed jets, the lateral spread of a compound angle film cooling jet increased, thus improving the laterally averaged effectiveness near the injection location. A significant improvement over streamwise directed jets was found at higher blowing ratio, $M \geq 1$ (all these studies were done at density ratio of $DR \approx 1$, so this corresponds to $I \geq 1$), which indicated that the jets stayed closer to the wall when a compound angle was used. However, far downstream the effectiveness results were different at higher M. Goldstein et al. (1970), who determined effectiveness from adiabatic wall temperature measurements, found that the improvement was sustained far downstream. Ligrani et al. (1992), who deduced adiabatic results from Stanton number extrapolations using superposition, found that the compound angle effectiveness decreased to the values for $CA = 0$ deg holes over a similar streamwise distance.

A computational study of a single row of laterally directed holes was conducted by Sathyamurthy and Patankar (1990), for a streamwise distance to $x/D = 10$ downstream of the holes. Rows of holes with $\beta = 30$ deg, $CA = 45$ and 90 deg, and with spacing between holes from $P/D = 3$ to 5 were investigated with unit density ratio injection. They stated that their analysis should be interpreted as qualitative since there are very limited experimental data with which to validate the computations. For $P/D = 3$ and $M = 1.0$ ($I = 1.0$), the laterally averaged effectiveness was found to improve with increase in compound angle, but at $P/D = 5$ there was very little difference for $CA = 0$, 45, or 90 deg. They also found that for laterally directed holes, the average effectiveness continued to increase with increase in blowing ratio up to $M = 3.0$ ($I = 9.0$), the maximum blowing ratio computed.

The shape of the film cooling hole is also an important geometric variable, but it has received limited attention in the literature. Goldstein et al. (1974) examined holes that had circular metering sections and were widened out at 10 deg near the exits. Makki and Jakubowski (1986) examined holes that had trapezoidal cross sections and were diffused in the direction of the mainstream flow. They used a transient facility, for which film cooling performance was indicated by the ratio of heat transfer coefficients with cooling to those without cooling. Both studies showed that expanding the hole exit improved film cooling performance compared to the round hole base case. However, there are no studies of the effects of compound angle with shaped or expanded holes in the open literature.

The effects of increasing hole spacings were discussed by Brown and Saluja (1979) and Foster and Lampard (1980) for streamwise-directed holes. Spacing of injection holes affects

Contributed by the International Gas Turbine Institute and presented at the 39th International Gas Turbine and Aeroengine Congress and Exposition, The Hague, The Netherlands, June 13–16, 1994. Manuscript received by the International Gas Turbine Institute February 9, 1994. Paper No. 94-GT-312. Associate Technical Editor: M. G. Dunn.

film cooling performance in two ways: The spacing determines the coolant mass per unit span at a given blowing condition, and closer spacing promotes jet merging, thus improving lateral coverage. There have been no studies reported for compound angle holes.

The customary way to describe film cooling performance defines the heat transfer coefficient in terms of adiabatic wall temperature, T_{aw}. In nondimensional form, T_{aw} is expressed as the adiabatic effectiveness. In the present experimental program, adiabatic effectiveness and heat transfer coefficients were determined for laterally directed film cooling holes, round and expanded, and for round streamwise-directed holes (as a basis for comparison). This paper presents the adiabatic effectiveness results. The associated heat transfer coefficients for the different hole configurations are presented in Sen et al. (1996).

Experimental Facilities and Techniques

Experiments were conducted in a closed-loop, subsonic wind tunnel facility, illustrated in Fig. 1. A secondary flow loop provided cryogenically cooled injection air to obtain the desired density ratio. Further details of the facility can be found in Pietrzyk et al. (1990). The flat test plate was a modular design composed of three sections: a 12.7-cm-long, sharp leading edge plate; a 14-cm-long injection plate; and an instrumented downstream plate. The sharp leading edge section had a 45 deg angle cut on the upstream edge. Suction at the leading edge, shown in Fig. 1, was adjusted so that a uniform flow with no separation occurred at the leading edge. The injection plate had a single row of holes with one of three different geometries to be described later. The geometry and coordinate system of the film cooled test plate is shown in Fig. 2.

This study considered three hole geometries, illustrated in Fig. 3, all with injection angle $\beta = 35$ deg, metering inlet diameter $D = 11.1$ mm, and a hole length of $L = 4D$. The test plates were constructed from extruded polystyrene foam (Styrofoam) with nine holes at a hole spacing of 3D; hole spacing was doubled by taping alternate holes closed. The basic geometry parameters of hole length, spacing, and injection angle were selected to be representative of the geometry used for turbine blade film cooling holes. Two compound angles were used: $CA = 0$ deg, with the hole axes aligned with the free-stream direction; and $CA = 60$ deg, with the hole axes at a 60 deg angle to the free stream. The $CA = 0$ deg holes were round holes and were tested as a basis of comparison. Two geometries were constructed with $CA = 60$ deg: a round hole case and a forward expanded exit case. The metering length, measured along the hole axis, was 2.1 D for the expanded exit holes, and the exit was expanded at a 15 deg angle along the line of the laterally directed hole as indicated in Fig. 3. Note that the projected cross-stream exit width of the expanded hole with $CA = 60$ deg was 3.3 D, which resulted in an overlapping of the projected widths, although the holes did not physically overlap.

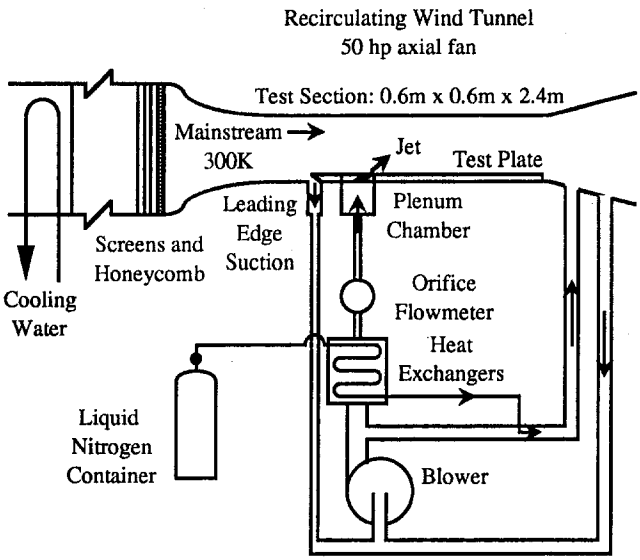

Fig. 1 Film cooling test facility

The 60 deg compound angle and 15 deg forward expansion angle were specified by Garrett Engine Division of AlliedSignal Aerospace and represent geometries in use in Garrett gas turbines. The hole inlets and exits were sharp edged, and the interiors were aerodynamically smooth. The holes were supplied by a common plenum, 48 cm by 12.7 cm in cross section (70 times the inlet area of all nine injection holes) and 48 cm deep, with several screens to promote more uniform flow through the plenum. The coolant temperature was monitored by a thermocouple positioned about 7 D below the entrances to the holes, which was found to give temperatures equivalent to the jet exit temperature.

The downstream plate was constructed from Styrofoam to provide an adiabatic boundary condition. A three-dimensional conduction heat transfer code indicated negligible conduction errors for this plate material (Sinha et al., 1991). The foam was bonded to a fiberglass composite (Extren) for structural rigidity. Below the Extren was 15.2 cm of Corning fiberglass insulation and 2.54 cm of Styrofoam. Surface roughness of the Styrofoam was measured to be less than 0.005 mm, which was much less than $y^+ = 5$ for the boundary layer flow on the test plate, so that the test plate was aerodynamically smooth.

An array of thin ribbon thermocouples was epoxied to the surface for surface temperature measurements. Because the thermocouple ribbons were very thin relative to their width, 38 μm thick and 1.5 mm wide, conduction error was negligible. An IR camera was used to verify that the thermocouple ribbons did not cause a smearing of the large temperature gradients that

Nomenclature

CA = compound angle
D = film cooling hole diameter
DR = density ratio of coolant to mainstream = ρ_c/ρ_∞
H = shape factor = δ_1/δ_2
I = momentum flux ratio of coolant to mainstream = $\rho_c U_c^2/\rho_\infty U_\infty^2$
L = hole length
M = mass flux ratio of coolant to mainstream = $\rho_c U_c/\rho_\infty U_\infty$
P = hole spacing
Re = Reynolds number
T = temperature
U = streamwise velocity
U_c = bulk cooling jet velocity through metering length of hole
x = streamwise coordinate originating at downstream edge of cooling holes
z = spanwise coordinate originating at centerline of central hole
β = angle of injection with respect to the surface
δ_1 = displacement thickness
δ_2 = momentum thickness
η = adiabatic effectiveness = $(T_{aw} - T_\infty)/(T_c - T_\infty)$
ρ = density

Subscripts

aw = adiabatic wall
c = coolant
∞ = free stream

Superscripts

$\bar{}$ = lateral average
$\bar{\bar{}}$ = spatial average

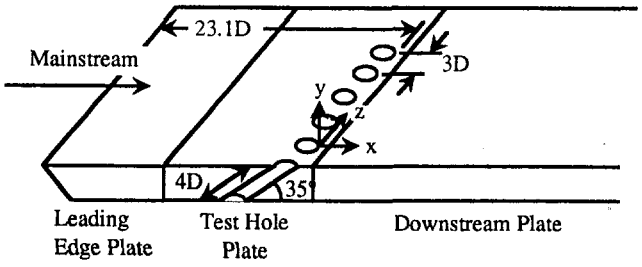

Fig. 2 Test section geometry and coordinate system

occurred during film cooling tests. The junctions formed by welding the ribbons were approximately 0.4 mm in diameter, and the ends of the ribbons were soldered to 0.5 mm thermocouple extension wires, which were routed through the test plate. The thickness of the thermocouple junctions after gluing to the surface ranged from 0.1 to 0.2 mm ($y^+ = 6$ to 12 at the highest velocity), which caused negligible aerodynamic interference. Further details about the thin ribbon thermocouple design are provided by Sinha et al. (1991). Nine thermocouple junctions were located on the central hole centerline from 2 D to 30 D downstream of the trailing edge of the hole. At streamwise locations of 3 D, 6 D, 10 D, and 15 D, seven thermocouple junctions were used, spanning the lateral distance from -1.5 D to $+1.5$ D. These lateral locations were for $P/D = 3$ hole spacing. For $P/D = 6$ spacing two runs were necessary to form a composite picture of the cooling jet performance. In these cases, with the central hole open and adjacent holes taped, data were obtained for -1.5 $D \leq z \leq 1.5$ D, and with the central hole taped and adjacent holes open data were obtained for 1.5 $D \leq z \leq 4.5$ D. Thermocouples were used to monitor free-stream and secondary loop temperatures. Acquisition of temperature data and data processing was automated to allow on-line analysis of film cooling effectiveness. Pressure differentials across the wind tunnel contraction and across a sharp-edged orifice plate in the secondary flow loop were used to set free-stream velocity and injection flow rate, respectively.

The operating technique utilized for this study was to set the mass flow rate of the cryogenically cooled injectant, then vary the free-stream velocity to obtain the desired blowing conditions. The coolant-to-mainstream density ratio and the blowing conditions were selected to be representative of the actual film cooling process. The free-stream velocity ranged from $U_\infty = 30$ m/s to 7.5 m/s, providing momentum flux ratios from $I = 0.16$ to 3.9 ($M = 0.5$ to 2.5), with $DR = 1.6$. A comprehensive description of free-stream and boundary layer development and uniformity was given by Pietrzyk et al. (1990) for a 20 m/s free-stream velocity. For this study the boundary layer profiles were measured immediately upstream of the film cooling holes (with no cooling flow), which was a position 21.6 cm downstream of the leading edge. The boundary layers were found to be fully developed turbulent boundary layers at $U_\infty = 20$ m/s and $U_\infty = 10$ m/s. The boundary layer parameters for $U_\infty = 20$ m/s were $\mathrm{Re}_{\delta 2} = 1100$, $\delta_1/D = 0.120$, and $H = 1.48$. At $U_\infty = 10$ m/s, the boundary layer parameters were $\mathrm{Re}_{\delta 2} = 700$, $\delta_1/D = 0.151$, and $H = 1.46$. These values were obtained without using a trip wire, and no trip wire was used for the effectiveness tests. The precision uncertainty on free-stream velocity was $\delta U_\infty = \pm 1$ percent, and the free-stream turbulence level was about $Tu = 0.2$ percent. The Reynolds number based on the free-stream velocity and the hole diameter ranged from $\mathrm{Re}_D = 5000$ to 21,000. The technique of varying free-stream conditions to obtain the various I and M ratios raised concerns about Reynolds number effects. Tests were conducted maintaining a constant I using several injectant mass fluxes and free-stream velocities for one geometry at one low I near the optimum performance condition, and one high I. The variation in the laterally averaged effectiveness was within the uncertainty of $\bar{\eta}$ for injection conditions spanning the range of Re_D.

Pietrzyk et al. (1990) also documented the film cooling loop. The cooling jets were supplied by a common plenum. Pietrzyk et al. performed laser-Doppler anemometry measurements of individual jets and found a mean velocity variation between jets of $\delta U_c = \pm 2.6$ percent. For the data described below, the mass flux ratio was held constant within $\delta M = \pm 4$ percent during experiments. The injectant-to-free stream density ratio was $DR = 1.6$. Maximum variation of density ratio between all experiments was $\delta DR = \pm 4$ percent, although the variation during any one experiment was $\delta DR = \pm 2$ percent. The free-stream temperature was allowed to vary ± 0.5°C and the coolant temperature was allowed to vary ± 2°C during an experimental run.

The low temperature of the dense jets meant a potential for H_2O and CO_2 to solidify and accumulate in the secondary flow loop and on the test plate. Wind tunnel air drying techniques and operating procedures developed by Pietrzyk et al. (1990) to reduce the frosting potential were employed. A new heat exchanger for cooling the jets was installed and the tunnel was sealed to minimize air infiltration to the wind tunnel, although a fully effective seal could not be obtained. This meant that frost could accumulate during an experiment, and it would have to be removed from the test plate between adiabatic effectiveness measurements. Repeated tests showed consistent performance was obtained after frost removal, with the variation in

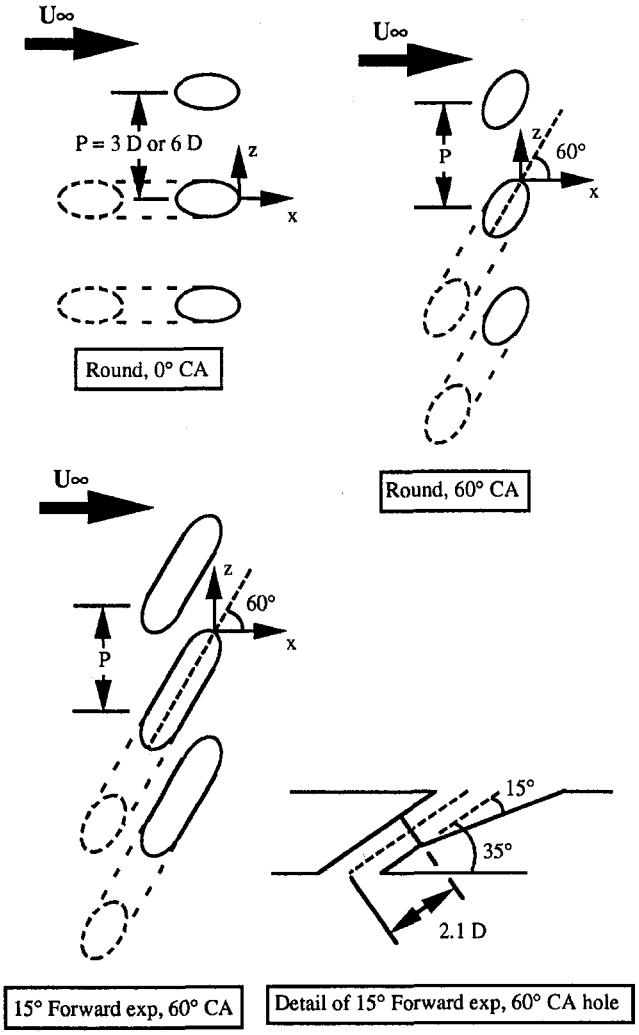

Fig. 3 Injection hole geometry showing the top view of the central three holes for all three geometries, and details of the geometry for the 15 deg forward expansion, 60 deg CA holes

local effectiveness, laterally averaged effectiveness, and spatially averaged effectiveness being $\delta\eta = \pm 0.01$, $\delta\bar{\eta} = \pm 0.01$, and $\delta\bar{\bar{\eta}} = \pm 0.01$, respectively.

Based on the uncertainties for flow conditions and freestream, coolant, and surface temperatures, and the uncertainties due to frost effects, the sequential perturbation technique (Moffat, 1988) was used to estimate the resulting uncertainties for adiabatic effectiveness values. We also obtained a direct measure of the precision uncertainties for adiabatic effectiveness by performing a number of repeatability tests. Most of these were performed with $CA = 0$ deg round holes for which six sets of measurements were made in four separate experiments conducted over a span of three years. The momentum flux ratio for these tests was $I = 0.16$, and similar repeatability tests were conducted with $I = 0.63$ and $I = 1.4$. Statistical analysis of the variation of the local values of η gave an uncertainty of $\delta\eta = 0.03$ for all momentum flux ratios and streamwise positions. The analysis of variations of laterally averaged and spatially averaged effectiveness gave uncertainties of $\delta\bar{\eta} = 0.02$ and $\delta\bar{\bar{\eta}} = 0.02$, for all streamwise positions and momentum flux ratios. The sequential perturbation analysis gave equivalent values for uncertainties for laterally and spatially averaged effectiveness, but a slightly lower value for local effectiveness. Similar uncertainties were obtained using compound angle holes, although not the same compound angle discussed in this paper.

In terms of percentages, the uncertainty of the local effectiveness ranged from 5 percent of the largest centerline value to 15 percent of the smallest centerline value for all data presented. The uncertainty for the laterally averaged effectiveness ranged from 5 to 20 percent for all data presented, except for round holes with $CA = 0$ deg and $P/D = 6$, in which case very low $\bar{\eta}$ values were obtained. For the spatially averaged effectiveness results, the uncertainty ranged from 7 to 20 percent for all data presented, except for round holes with $CA = 0$ deg data at $I > 1.0$, in which case the coolant jets were completely separated, resulting in very low effectiveness values.

The evaluation of film cooling performance discussed below refers to blowing ratio and momentum flux ratio. These ratios are defined using the injectant velocity, U_c, based on the flow rate and the cross section area of the metering length (inlet) of the hole. Studies reported in the literature commonly use the jet velocity in the definitions of M and I. However, expanding the hole exit increases the cross-sectional area after the metering length, hence the jet velocity decreases. In this situation, U_c is used in the description of flow conditions since the correct representative jet velocity is not known.

Results and Discussion

Results for the three hole geometries tested are presented in terms of lateral variations of local effectiveness η, streamwise variation of laterally averaged effectiveness $\bar{\eta}$, and finally the variation of spatially averaged effectiveness $\bar{\bar{\eta}}$ as a function of momentum flux ratio. The results of the 3 D and 6 D hole spacings are presented together to aid in the description of the effects of compound angle injection. For the coordinate system we placed the streamwise coordinate origin, $x = 0$, at the trailing edge of the film cooling hole. The lateral coordinate origin, $z = 0$, was at the centerline of the trailing edge of the central hole. The coordinate system origins are shown in Fig. 3 for each geometry.

The validity of the round hole $CA = 0$ deg results was established by comparing the effectiveness with results from Pedersen et al. (1977) and results from Sinha et al. (1991). Both studies measured effectiveness at high density ratio and had injection geometries similar to the present study, although the injection hole lengths were substantially different. The present study used holes with $L/D = 4.0$, while Pedersen et al. used much longer holes ($L/D \sim 40$) and Sinha et al. used holes with $L/D = 1.75$. For low I, there was good agreement between the present results and the data of Pedersen et al. and Sinha et al., as illustrated by the centerline data in Fig. 4(a). At high I (Fig. 4(b)), for which jet lift-off occurs in the near-hole region, the present results showed some deviation from the data of Pedersen et al. and Sinha et al. The difference was primarily attributed to differences in the film cooling hole length-to-diameter ratio for the different studies.

The lateral movement of the cooling jet expected for compound angle injection is clearly illustrated by comparing in Figs. 5(a) and 5(b), which show lateral η distributions at the four streamwise stations for the round holes with $CA = 0$ and 60 deg. A distinct difference in the initial lateral distribution of coolant for the round holes and expanded exit holes with compound angle is evident when comparing Figs. 5(a), 5(b), and 5(c). The expanded exit holes have an almost uniform lateral distribution of coolant at the first measurement position of $x/D = 3$, while the round holes show a large lateral variation. However, by $x/D = 15$ both round and expanded exit holes with compound angle show similar uniform lateral distributions.

We selected $x/D = 10$ as a representative position for the following comparisons of the lateral distribution of η for the different hole geometries. Results presented in Fig. 6 are representative of low momentum flux ratio ($I < 0.5$), and results presented in Fig. 7 are representative of high momentum flux ratio ($1 \leq I < 4$). Figure 6(a) shows that $\eta > 0.1$ across the span between holes for low I and for $P/D = 3$. This result suggests that there is some merging of the coolant jets for all hole geometries for this hole spacing. For $P/D = 6$, Fig. 6(b) shows a distinct region of zero effectiveness indicating the coolant jets no longer merged (note, data were not taken for $z/D > 1.5$ for round $CA = 0$ deg and the round $CA = 60$ deg holes because it was evident that η would be essentially zero over this range). Also evident from Fig. 6(b) is that the forward expanded $CA = 60$ deg holes deliver a much greater lateral distribution of the coolant. At high I, Fig. 7(a) shows that the round and the forward expanded $CA = 60$ deg holes have similar good lateral distribution of coolant for $P/D = 3$, and both are

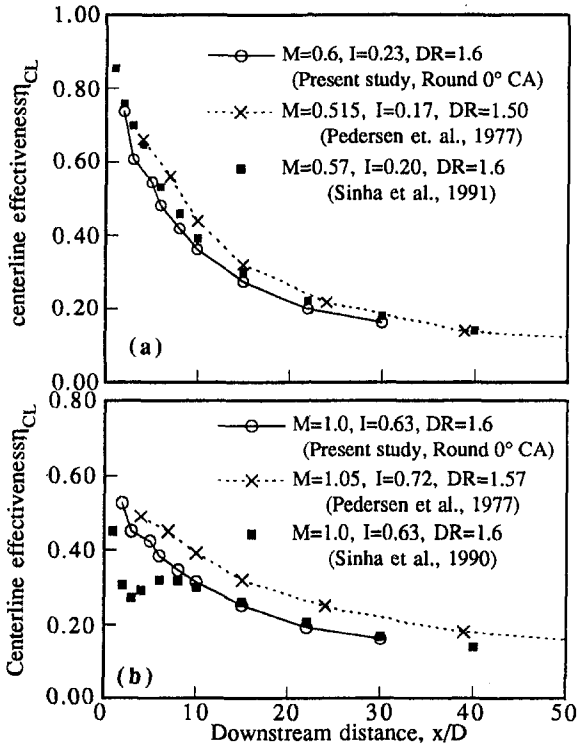

Fig. 4 Comparison of round hole centerline effectiveness to published data: (*a*) $I = 0.23$, $M = 0.6$, (*b*) $I = 0.63$, $M = 1.0$

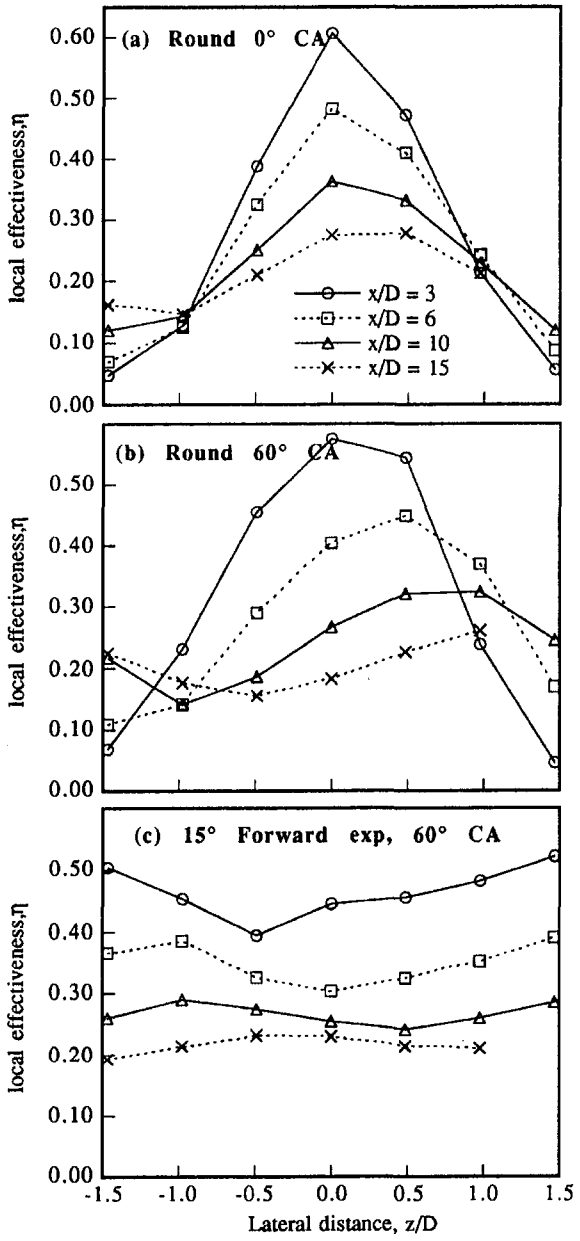

Fig. 5 Local lateral effectiveness for the holes with CA = 60 deg, I = 0.25, M = 0.63

clearly superior to the round CA = 0 deg holes. However, for P/D = 6, Fig. 7(b) shows regions of zero effectiveness, indicating that the coolant jets have not merged, but there is a greater lateral distribution of coolant for both the round and forward expanded compound angle holes. Note that in Fig. 7(b) both compound angle cases also exhibited steep η gradients on the side toward which the jets were directed. We attribute this to the impact of the mainstream on this side of the jet causing a sharp shear layer.

Laterally averaged effectivenesses were determined by integrating the measured lateral distribution of η and dividing by the span between hole centerlines. A simple trapezoidal integration was used since it was found to give the same result as higher order polynomial fits. Results are shown as a function of downstream distance for $I \approx 0.25$ and $I \approx 1.0$ in Figs. 8 and 9, respectively. At the lower I, adding a compound angle to the round hole did not significantly change $\overline{\eta}$ compared to the base case round hole. In contrast, the combination of compound angle with the forward expanded exit caused a significant increase immediately downstream of the hole, but fell to a level equivalent to the round holes by x/D = 10. The initial improved $\overline{\eta}$ value for the forward expanded CA = 60 deg may be attributed to the improved lateral distribution of the coolant discussed previously. Increasing the spacing between holes from P/D = 3 to P/D = 6 caused approximately a factor of two decrease in $\overline{\eta}$, and $\overline{\eta}$ values for each of the holes were very similar.

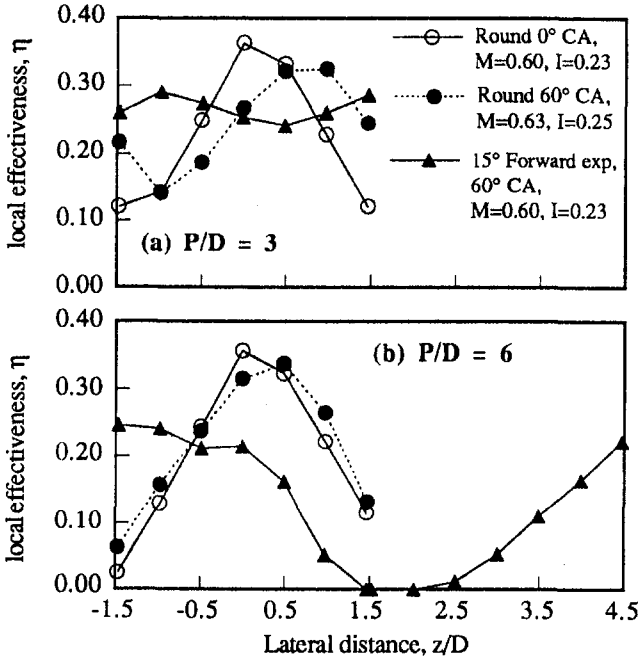

Fig. 6 Local lateral effectiveness at x/D = 10 for the test holes, $I \approx 0.25$, $M \approx 0.6$

Figure 9 shows that at relatively high I, there were distinct differences in the effectiveness for the different hole geometries. Both compound angle holes had significantly greater effectiveness than the baseline case round hole with CA = 0 deg. This is mainly because of a large decrease in $\overline{\eta}$ for the CA = 0 deg

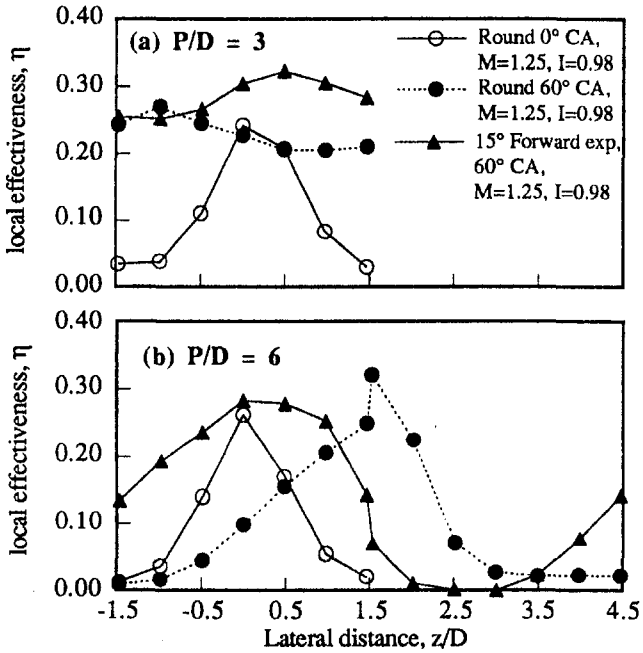

Fig. 7 Local lateral effectiveness at x/D = 10 for the test holes, I = 0.98, M = 1.25

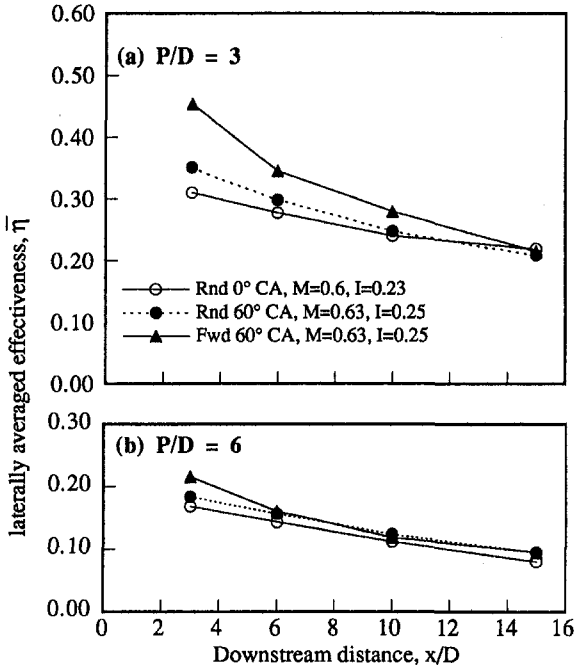

Fig. 8 Laterally averaged effectiveness for the test holes, $I \approx 0.25$, $M \approx 0.6$

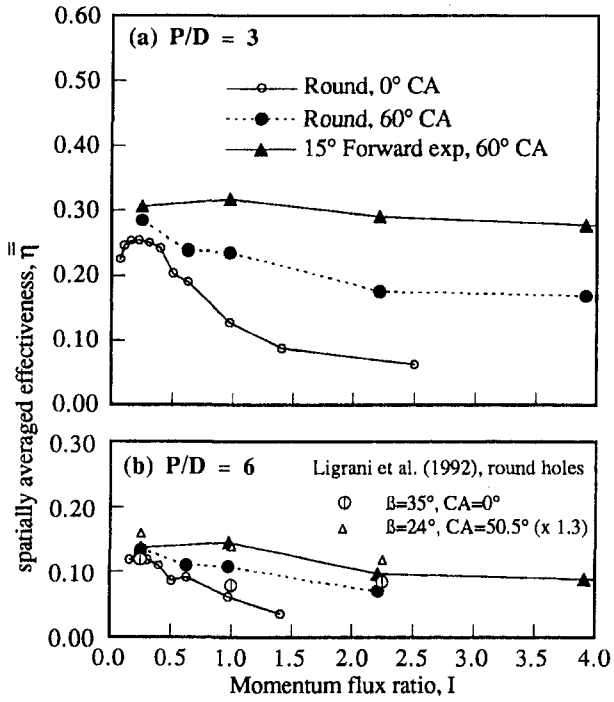

Fig. 10 Spatially averaged effectiveness for the test holes with $DR = 1.6$

round hole, which may be attributed to detachment of the cooling jet from the surface. Detachment of the cooling jet for $CA = 0$ deg round holes at $I = 1.0$ is consistent with the results of Thole et al. (1992), who showed that the coolant jet would be fully detached for $I > 0.8$. Again the forward expanded exit with $CA = 60$ deg significantly increased $\bar{\eta}$ immediately downstream of the holes, but fell to a level comparable to the round $CA = 60$ deg holes by $x/D = 15$. When the hole spacing was doubled, $\bar{\eta}$ was reduced by a factor of two, but the $CA = 60$ deg geometries retained significantly increased effectiveness relative to the $CA = 0$ deg holes.

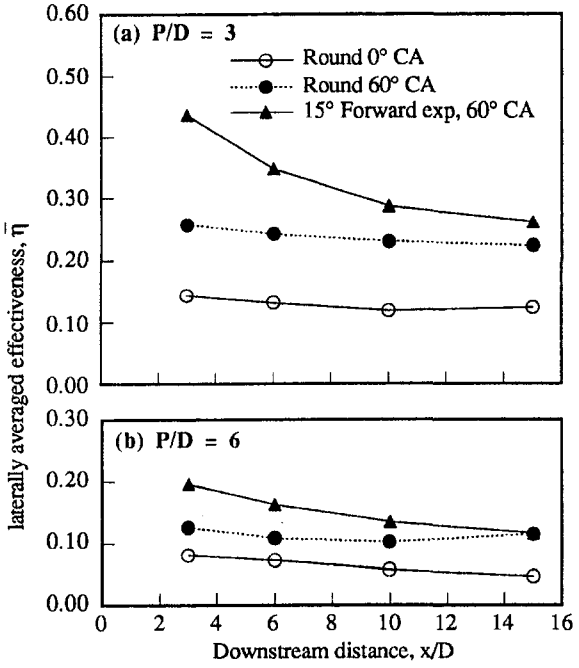

Fig. 9 Laterally averaged effectiveness for the test holes, $I = 0.98$, $M = 1.25$

To compare the effectiveness of the different geometries over a full range of momentum flux ratios, a spatially averaged adiabatic effectiveness, $\bar{\bar{\eta}}$, was used. This quantity was defined as the integral average of the laterally averaged effectiveness from $x/D = 3$ to 15. Results for $\bar{\bar{\eta}}$ for all three geometries as a function of momentum flux ratio are shown in Fig. 10. Immediately obvious from Fig. 10(a) for $P/D = 3$ is that the effectiveness at low I is very similar for the different geometries, but adding a 60 deg compound angle significantly increased the range over which high effectiveness levels were maintained. The forward expanded exit holes with $CA = 60$ deg maintained essentially the same level of $\bar{\bar{\eta}}$ over the full range tested, $0.25 < I < 3.9$, and were significantly better than the round $CA = 60$ deg holes at the larger I. For the round $CA = 60$ deg holes, $\bar{\bar{\eta}}$ decreased slightly with increasing I, but still had reasonably good effectiveness at $I = 3.9$. This decreasing trend for the $CA = 60$ deg round holes is somewhat different from the computational predictions of Sathyamurthy and Patankar (1990), which indicated a constant level of effectiveness for $CA = 45$ deg round holes, and increasing effectiveness with increasing I for $CA = 90$ deg round holes.

The effect of increasing hole spacing to $P/D = 6$ is shown in Fig. 10(b). Both round hole geometries had blowing conditions at which local lateral data for $1.5 < z/D < 4.5$ were not obtained (as noted previously, it was evident that η was essentially zero over this range). For these cases, averaged effectiveness results were calculated assuming $\eta = 0$ over $1.5 < z/D < 4.5$. The results for $P/D = 6$ are somewhat similar to the $P/D = 3$ results with the $\bar{\bar{\eta}}$ levels generally decreased by a factor of two. Results for the round holes with $CA = 0$ and 60 deg can be compared with the results of Ligrani et al. (1992), who used round holes with $CA = 0$ and 50.5 deg, but with an injection angle of $\beta = 24$ deg. The magnitudes of the effectiveness deduced from the data of Ligrani et al. over the range $x/D = 5$ to 15 were very similar to the present results for the range that Ligrani et al. tested, $0.25 < I < 2.2$. Similarly they found that the effectiveness of the compound angle round holes decreased with increasing I, but improved relative to the $CA = 0$ deg holes.

Conclusions

All three geometries had very similar spatially averaged adiabatic effectiveness at low momentum flux ratio, although the forward expansion with $CA = 60$ deg holes had an improved lateral spread of the film cooling jets immediately behind the holes. Adding a compound angle to the baseline round hole geometry significantly improved effectiveness at high momentum flux ratios, and the combination of compound angle and forward expansion provided further improvement. With a hole spacing of $P/D = 3$, the forward expanded $CA = 60$ deg holes maintained essentially the same level of spatially averaged effectiveness for the range of I studied, while the effectiveness level of the round $CA = 60$ deg holes decreased slightly with increasing I. The higher spatially averaged effectiveness obtained for the forward expanded holes was due to significantly higher effectiveness very near the hole, but by $x/D = 15$ the forward expanded and round $CA = 60$ deg holes had essentially the same effectiveness. With $P/D = 6$, both compound angle geometries retained significantly improved effectiveness compared to the streamwise directed round holes. These results indicate that film cooling with compound angle injection does not provide higher adiabatic effectiveness at the optimum momentum flux ratio, but does provide high effectiveness over a considerably larger range of momentum flux ratios. However, these adiabatic effectiveness results must be coupled with the heat transfer coefficients to determine overall performance as discussed in Sen et al. (1996).

Acknowledgments

The authors gratefully acknowledge Garrett Engine Division of the AlliedSignal Aerospace Company and the Air Force Wright-Patterson Research and Development Center for support of this research. We would also like to thank Mr. Noor Sait, Mr. David Dotson, and Dr. Karen Thole for their assistance in conducting experiments.

References

Brown, A., and Saluja, C. L., 1979, "Film Cooling From a Single Hole and a Row of Holes of Variable Pitch to Diameter Ratio," *International Journal of Heat and Mass Transfer,* Vol. 22, pp. 525–533.

Foster, N. W., and Lampard, D., 1980. "The Flow and Film Cooling Effectiveness Following Injection Through a Row of Holes," ASME *Journal of Engineering for Power,* Vol. 102, pp. 584–588.

Goldstein, R. J., Eckert, E. R. G., Eriksen, V. L., and Ramsey, J. W., 1970, "Film Cooling Following Injection Through Inclined Circular Tubes," *Israel Journal of Technology,* Vol. 8, pp. 145–154.

Goldstein, R. J., Eckert, E. R. G., and Burggraf, F., 1974, "Effects of Hole Geometry and Density on Three-Dimensional Film Cooling," *International Journal of Heat and Mass Transfer,* Vol. 17, pp. 595–607.

Honami, S., Shizawa, T., and Uchiyama, A., 1994, "Behavior of the Laterally Injected Jet in Film Cooling: Measurements of Surface Temperature and Velocity/Temperature Field Within the Jet," ASME JOURNAL OF TURBOMACHINERY, Vol. 116, pp. 106–112.

Ligrani, P. M., Ciriello, S., and Bishop, D. T., 1992, "Heat Transfer, Adiabatic Effectiveness, and Injectant Distributions Downstream of a Single Row and Two Staggered Rows of Compound Angle Film Cooling Holes," ASME JOURNAL OF TURBOMACHINERY, Vol. 114, pp. 687–700.

Makki, Y. H., and Jakubowski, G. S., 1986, "An Experimental Study of Film Cooling From Diffused Trapezoidal Shaped Holes," Paper No. AIAA-86-1326.

Moffat, R. J., 1988, "Describing Uncertainties in Experimental Results," *Experimental Thermal and Fluid Science,* Vol. 1, pp. 3–17.

Pedersen, D. R., Eckert, E. R. G., and Goldstein, R. J., 1977, "Film Cooling With Large Density Differences Between the Mainstream and the Secondary Fluid Measured by the Heat–Mass Transfer Analogy," ASME *Journal of Heat Transfer,* Vol. 99, pp. 620–627.

Pietrzyk, J. R., Bogard, D. G., and Crawford, M. E., 1990, "Effects of Density Ratio on the Hydrodynamics of Film Cooling," ASME JOURNAL OF TURBOMACHINERY, Vol. 112, pp. 437–443.

Sathyamurthy, P., and Patankar, S. V., 1990, "Prediction of Film Cooling With Lateral Injection," AIAA/ASME Thermophysics and Heat Transfer Conference, Seattle, WA.

Sen, B., Schmidt, D. L., and Bogard, D. G., 1996, "Film Cooling With Compound Angle Holes: Heat Transfer," ASME JOURNAL OF TURBOMACHINERY, Vol. 118, this issue, pp. 800–806.

Sinha, A. K., Bogard, D. G., and Crawford, M. E., 1991, "Film Cooling Effectiveness Downstream of a Single Row of Holes With Variable Density Ratio," ASME JOURNAL OF TURBOMACHINERY, Vol. 113, pp. 442–449.

Thole, K. A., Sinha, A. K., Bogard, D. G., and Crawford, M. E., 1992, "Mean Temperature Measurements of Jets With a Crossflow for Gas Turbine Film Cooling Application," in: *Rotating Machinery Transport Phenomena,* J. H. Kim and W. J. Yang, eds., Hemisphere Pub. Corp., New York.